Online coupling of a catalytic continuous microflow reactor to mass spectrometry

Hermans, Jos; Najmi, Ali Alipour; Permentier, Hjalmar; Bischoff, Rainer

Published in:
Talanta

DOI:
10.1016/j.talanta.2023.124928

Publication date:
2024

Talanta 266 (2024) 124928

Contents lists available at ScienceDirect

Talanta

journal homepage: www.elsevier.com/locate/talanta

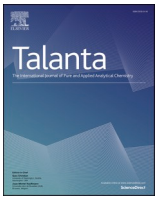

Online coupling of a catalytic continuous microflow reactor to mass spectrometry

Jos Hermans, Ali Alipour Najmi, Hjalmar Permentier, Rainer Bischoff *

Department of Analytical Biochemistry, Groningen Research Institute of Pharmacy, University of Groningen, Antonius Deusinglaan 1, 9713 AV, Groningen, the Netherlands

ARTICLE INFO

Handling editor: Qun Fang

Keywords:
Continuous flow catalysis
Dealkylation
Reaction mechanism
Adsorption/desorption profile
Gold micro particles

ABSTRACT

Flow cell reactors used for catalyst development and applications are upcoming due to their small environmental and economic footprint. Online microflow reactor coupling with mass spectrometry (MS) opens new possibilities for monitoring catalyst performance and identifying reaction products in real time. This is demonstrated for the metabolic relevant dealkylation of lidocaine on catalytic gold micro-particles using regular liquid chromatography modules. Yields of up to 90% norlidocaine were realized under mild continuous flow conditions for up to 10 h (pH 7, 30 °C and 20 μL/min). Dissolved oxygen was shown to be a rate-limiting factor, since an inline oxygen generator allowed to increase the reactor capacity by one order of magnitude. Monitoring product time-response curve slopes after starting and ending a substrate feed, provided insights into the adsorption/desorption and conversion kinetics at the catalyst surface indicating the presence of strong adsorption sites that do not contribute substantially to substrate conversion.

1. Introduction

Continuous-flow reactors are increasingly used for the synthesis of fine chemicals and active pharmaceutical ingredients in an effort to minimize waste, enhance (energy) efficiency and improve safety. When applied as a microreactor and combined with plug-flow injections, they also offer excellent high-throughput screening possibilities of reaction conditions [1,2]. Direct coupling of a microreactor to an analytical detector accelerates the optimization as well as the product identification and the catalyst characterization process by enabling online signal monitoring [3]. Coupling microreactors to MS is particularly advantageous as it allows the reliable identification and quantification of a wide range of organic compounds [4,5] opening the door to investigate reactions on heterogeneous and supported homogeneous (bio)-catalysts. Microreactors in microfluidic systems are often used to control the synthesis and characterization of nanoparticle catalysts [6], although clean room facilities are needed for their production. Packed-bed microreactors using regular capillaries provide the possibility to investigate heterogeneous catalysts in a more straightforward way due to their ease of implementation and fabrication using, for example, regular high performance liquid chromatography (HPLC) systems. Continuous flow reactors are available for regular [7], electro-chemical [8] as well as catalytic [9] reactions. In the following, we will focus on catalysis using gold particles as an example. Traditionally, gold is considered to be rather inert but its application in the form of homogeneous Au(I)- or Au(III)-catalytic complexes is ever growing, covering a wide range of reactions [10]. Heterogeneous gold catalysts are mainly used for industrial scale, gas-phase reactions such as the oxidation of CO to CO_2 in exhaust fumes using (supported) nanoparticles [11]. Application of larger diameter particles to more complex substrate molecules in the liquid phase is less common. We have previously shown that certain drugs can be dealkylated in the liquid phase using nanoporous gold in a batch cell set-up [12]. Dealkylation is one of a number of Phase-I metabolic oxidation reactions catalyzed by members of the Cytochrome P450 enzyme family. It is assumed that the critical step of this reaction is the formation of a perferryl intermediate (FeO_3^+) during the uptake of molecular oxygen by the enzyme [13]. The perferryl intermediate is thought to generate reactive oxygen species (ROS) by serving as an electron sink and as a binding site for molecular oxygen facilitating oxygen activation by electron transfer reactions [14,15].

In the current work we describe a modular online Au-catalyst-MS system to study the deethylation of lidocaine performing plug-flow injection as well as continuous-flow experiments. The modular system allowed us to study and optimize the reaction by including an ‘oxygen

* Corresponding author.
E-mail address: r.p.h.bischoff@rug.nl (R. Bischoff).

https://doi.org/10.1016/j.talanta.2023.124928
Received 22 May 2023; Received in revised form 5 July 2023; Accepted 7 July 2023
Available online 11 July 2023

generator' based on a MnO_2-reactor and by performing post-reactor derivatizations to study the reaction mechanism, for example for the detection of acetaldehyde (Scheme 1). Our online microflow catalyst-MS system can be adapted to study other heterogeneous catalysts as well as other chemical reactions with a minimal consumption of chemicals.

2. Materials and methods

2.1. Chemicals and materials

Free base lidocaine and caffeine standards (Merck, Amsterdam, The Netherlands) were prepared in Milli-Q water and stored at 4 °C. Acetonitrile, methanol and isopropanol (Biosolve, Valkenswaard, The Netherlands) were used as organic solvents. Ammonium bicarbonate, formic acid, ammonium sulphite, hydrogen peroxide and ^{18}O-water (98%) (Merck, Amsterdam, The Netherlands) were used as additives or additional reagents.

2.2. Equipment

For the instrumental set-up given in Fig. 1, several Agilent series 1100 capillary HPLC components (Waldbronn, Germany) were used comprising two binary microflow pumps with stream splitter and flow controller (20 µL/min), one isocratic pump, a thermostatic autosampler (10 °C) and a thermostatic column/reactor compartment (10–80 °C) equipped with a 6-port switching valve. The Au- and MnO_2-reactors were homemade from peek tubing (Merck, Amsterdam, The Netherlands). The Au-reactor was 0.76 mm × 68 mm filled with 387 mg of 15–37 µm 18 K white gold particles (BO1947714, Cookson Drijfhout, Amsterdam, The Netherlands) and the MnO_2-reactor was 0.76 mm × 55 mm filled with 47 mg of 1 µm MnO_2 particles (Merck, Amsterdam, The Netherlands). Both reactors were sealed with 0.5 µm frits (IDEX Health and Science, Oak Harbor, USA). Reaction products were detected by mass spectrometry using a TSQ Quantum Discovery Max triple quadrupole mass spectrometer (ThermoFisher Scientific, Breda, The Netherlands) equipped with an electrospray source operated in positive ionization mode. Data were acquired between *m/z* 70–350 with a spray voltage of 3000 V, a capillary temperature of 315 °C and sheath and aux gas pressures of, respectively, 21 and 4. Selected reaction monitoring (SRM) was used operating in negative mode to analyze sulfonated acetaldehyde at the *m/z* transition 125/81 with a collision energy of 7 eV using the same ion-source settings at a spray voltage of −4000 V. Xcalibur 4.1 software was used for data acquisition and processing.

2.3. Plug flow injection optimization

Operational parameters were optimized with plug-flow injections of lidocaine and the Au-reactor configured as shown in Fig. 1 without the MnO_2-reactor. Initial and final parameter settings and ranges are given in Table 1. Plug-flow injections start with water (solvent A) from pump 1. After 10 min, the reactor is cleaned with 0.1% formic acid in acetonitrile (solvent B) from pump 2. After an additional 5 min, the reactor is reconditioned with water (solvent A from pump 1) for 15 min, which concludes the run. For injection plugs of more than 20 µL, the initial isocratic period was extended by 5 min for each additional 20 µL up to the maximum loop volume of 40 µL. Pump 3 delivered 0.1% formic acid

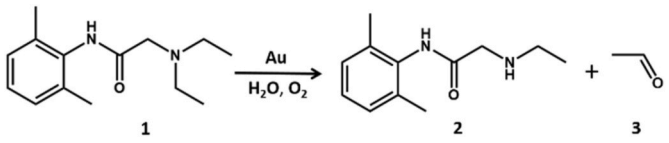

Scheme 1. Catalytic deethylation of lidocaine on gold particles in the presence of molecular oxygen. Lidocaine (1) is deethylated to norlidocaine (2) with production of acetaldehyde (3).

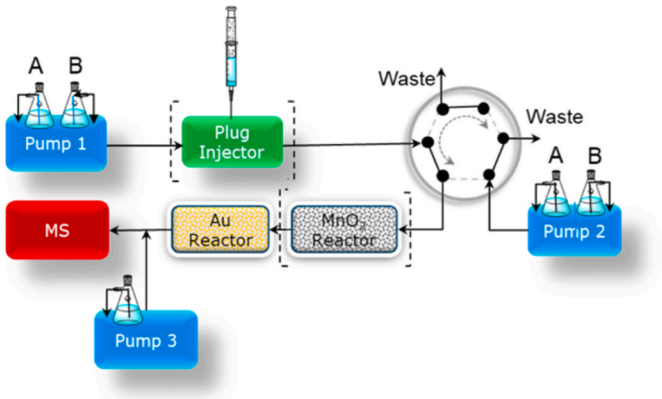

Fig. 1. Instrumental set-up for continuous- or plug-flow injections over the catalytic Au-reactor online coupled to a mass spectrometer. The elements in brackets are optional and used depending on the respective experiment. Operational parameters are given in Table 1.

Table 1
Initial, optimal and parameter ranges for evaluating the Au-reactor.

Parameter	Initial	Range	Optimal
Volume(µL)	1	1–40[a] 20–7200[b]	1200[b]
Flow (µL/min)	20	1–20	20
Temperature (°C)	25	10–80	30
pH	8	3–8	7-8
Lidocaine (µL)	100	1–1000	10
Solvent	H_2O	H_2O/ACN	H_2O

[a] Plug flow.
[b] Continuous flow.

in 50% acetonitrile at 50 µL/min as a make-up flow to stabilize the electrospray.

To evaluate the influence of pH, solvents A and B from pump 1 were respectively filled with 0.01% formic acid and water, covering a pH range from 3 to 7 by mixing both solvents at 0, 1, 10, 20, 25, 30, 50 and 100% B. Experiments at pH 8 were performed using 5 mM ammonium bicarbonate in water.

2.4. Continuous flow optimization

Additional optimization experiments were performed in continuous-flow mode by changing the temperature (10–80 °C) and the solvent composition (0–90% acetonitrile in water) at 10 µM lidocaine. Different Au-reactor cleaning and/or regeneration conditions were evaluated by filling bottles A and B from pump 2 with water (A), acetonitrile, methanol or isopropanol (B) with and without 0.1% formic acid. The influence of substrate concentration was evaluated for 16 min under continuous-flow conditions at 20 µL/min (320 µL) using 100 or 1000 µM lidocaine in bottle A from pump 1 and water from bottle B across a range of 1–1000 µM by mixing both solvents accordingly.

2.5. Quantitation

Quantitative measurements were performed by analyzing 100 µL fractions from continuous flow feeds through the reactor under optimal conditions (Table 1) by performing reverse phase chromatography over a 2 × 150 mm 3 µm XBridge C18 column at 300 µL/min using full scan mass spectrometry (*m/z* 70–350). The gradient started 2 min after the injection from 2% acetonitrile reaching 25% 4 min later, increased further to 80% during in 1 min, staying at 80% for another minute and going back to 2% in 1 min finishing the run after 12 min in total. The system was calibrated with a calibration line in the range of 1–200 µM

for lidocaine and norlidocaine using caffeine at 50 μM for normalization.

2.6. Mechanism confirmation

2.6.1. Involvement of molecular oxygen

Addition of 5 mM $(NH_4)_2SO_3$ to solvent A from pump 1 was used to completely remove dissolved molecular oxygen by oxidizing sulfite to sulfate, (Eq (1)).

$$2SO_3^{2-} + O_2 \rightarrow 2SO_4^{2-} \quad (1)$$

2.6.2. Oxygen enrichment conditions

Oxygen-enriched conditions were created by sandwiching 1–16 μL 100–1000 μM lidocaine plugs between two 8 μL10 mM hydrogen peroxide plugs and running them over a MnO_2-reactor in series with the Au-reactor (Fig. 1), (Eq (2)). The generated molecular oxygen remains in solution due to the closed system having an overall pressure of about 40 bar. Continuous oxygen enrichment was realized by the introduction of a fourth pump leading 100 mM hydrogen peroxide over a MnO_2-reactor at a flow of 4 μL/min to the main liquid stream of 20 μL/min as depicted in Figure S1

$$2H_2O_2 \xrightarrow{MnO_2} 2H_2O + O_2 \quad (2)$$

2.6.3. Involvement of water

Acetaldehyde, one of the proposed reaction products (see Scheme 1), was identified according to Hu et al. [16] using plug flow injections and negative electrospray ionization MS with online, post-reactor derivatization using 5 mM ammonium sulfite (Eq 3) in 50% acetonitrile added from pump 3 at 50 μL/min (Fig. 1). The dealkylation reaction was performed with lidocaine in ^{18}O-water to assess the involvement of water monitoring the production of ^{18}O-acetaldehyde(sulfonate).

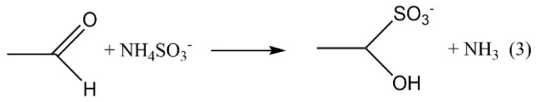

2.7. Adsorption/desorption profile

Continuous flow experiments were performed with the set-up shown in Fig. 1 without both components in brackets. Runs at 20 μL/min start with water from pump 1, followed after 5 min by a valve switch for 0, 1, 2, 4, 8, 16 or 32 min to effectuate a 10 μM lidocaine/caffeine mixture plug injection in water (solvent A) from pump 2. Caffeine is used as a reference compound that is not adsorbed to nor converted by the Au-catalyst. Hereafter, the valve is switched back eluting the reactor with water from pump 1 for 20 min followed by a 5 min cleaning step with 0.1% formic acid in acetonitrile from pump 2 (solvent B). The run is completed by switching back to pump 1 and reconditioning the reactor with water for 16 min.

3. Results and discussion

3.1. Plug-flow optimization

The optimization process started with plug-flow injections with the goal to find conditions giving the highest deethylation yield with a minimum of byproducts as summarized in Table 1. A time-response plot of all detectable extracted [M+H] + ion signals of lidocaine and its conversion products is represented in Fig. 2a for 16 μL plug-flow injections. Fractions representing the breakthrough with water, cleaning with 0.1% formic acid in acetonitrile and reconditioning with water are indicated as 'break', 'clean' and 'condition' in Fig. 2b and c. The plots illustrate the absence of lidocaine (1) (*m/z* 235) in the breakthrough fraction, which is dominated by the deethylated product norlidocaine (2) (*m/z* 207). This fraction also contains a byproduct at *m/z* 233, which

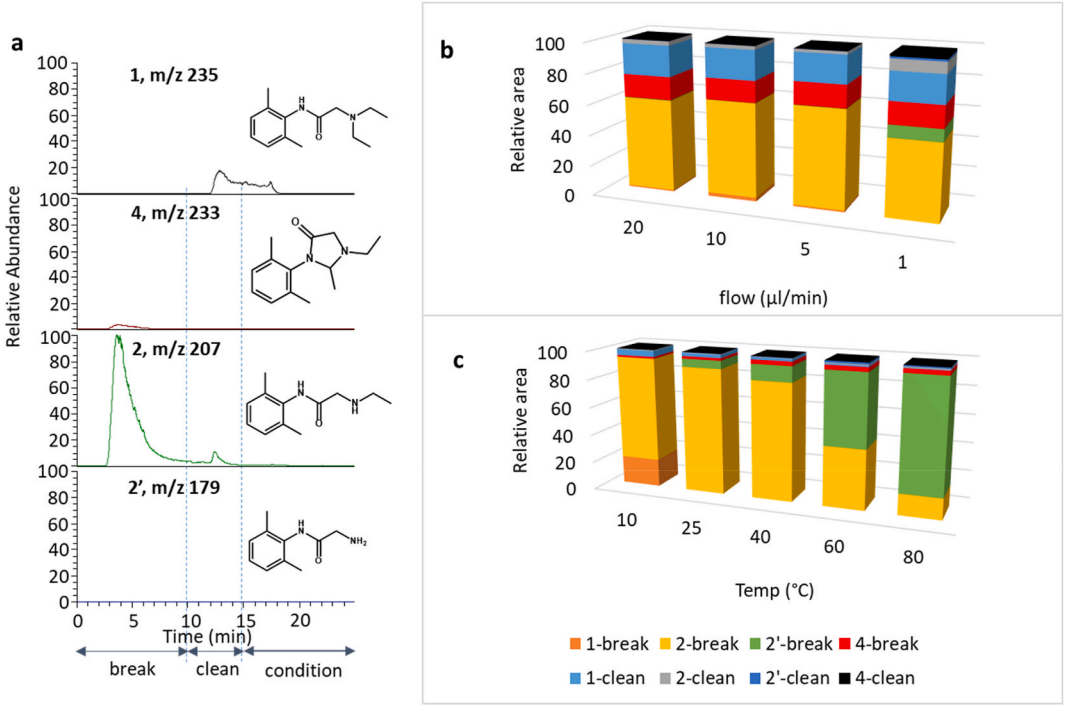

Fig. 2. (a) Extracted ion chromatograms of all observed conversion products upon 16 μL 100 μM lidocaine (1) plug-flow injections over the Au-reactor showing that norlidocaine (2) is the main product under optimal conditions (intensity scales are equal). Influence of (b) flow-rate and (c) reactor temperature on product distribution as depicted in relative peak areas showing that elevated temperatures lead to more di-deethylation (2′) while flow-rates down to 5 μL/min do not affect product distribution significantly.

was identified as a cyclized form of lidocaine (4) [12]. Increasing the percentage of organic solvents like methanol or acetonitrile in water led to reduced conversion, with no conversion at all in the absence of water. The reaction did not proceed either at pH values below 3.5 (Figure S2). Most subsequent experiments were thus performed in water between pH 7 and 8.

Although hardly detected under optimized conditions, the byproduct di-deethylated lidocaine (2′) is produced at increased reactor contact time (decreasing flow-rate) and temperature as illustrated by the green bars in Fig. 2b and c. The production of norlidocaine (2) was slightly reduced in favor of di-deethylated lidocaine (2′) at the lowest flow-rate, corresponding to a contact time of 2 min. The rather stable product ratios at higher flow-rates indicate that conversion is fast. Considering an estimated Au-reactor void volume of 2 μL, the contact time of injection plugs is between 0.1 and 2 min for flow-rates of 20 to 1 μL/min. This translates into a conversion rate of more than 2 nmol/min at the maximum flow-rate of 20 μL/min infusing 100 μM lidocaine. Experiments were continued at this flow-rate to limit the analysis time, although lower flow-rates may allow for plug injections at higher concentrations. The optimum reactor temperature for producing norlidocaine (2) was between 20 and 40 °C (Fig. 2c). At 10 °C lidocaine (1) starts to break through due to a reduced reaction rate while at higher temperatures the reaction proceeds further producing mainly di-deethylated lidocaine (2') at 80 °C.

The estimated relative conversion of lidocaine in the plug flow experiments under optimized conditions was close to 100%. This was confirmed by the quantitative measurements described at section 2.5 which also showed that norlidocaine has an almost two times lower response factor in ESI-MS than lidocaine (Figures S3 & S4).

3.2. Continuous flow catalysis

The effect of increasing plug volumes was investigated in preparation for continuous-flow experiments. Lidocaine plugs from 1 to 40 μL at 100 μM showed stable conversions producing 80–100% norlidocaine at 20 μL/min and 25 °C (Figure S4). Higher plug volumes of up to 0.6 mL (30 min at 20 μL/min) at 100 μM required elevated temperatures up to 80 °C to prevent a decline in conversion without inducing extensive di-deethylation as observed with small plugs (Figure S5). Continuous-flow experiments over several hours at 25–40 °C were performed at 10 μM lidocaine. Changing the operational parameters under these conditions allowed us to monitor product and by-product formation in real-time (Fig. 3). Lowering the temperature from 25 to 10 °C led to a reduction in lidocaine conversion by more than 50%. The optimal temperature lies in the range of 30–40 °C. Continuous monitoring of extracted ion chromatograms was also helpful in optimizing cleaning of the catalyst. This showed for example, that 0.1% formic acid in acetonitrile is superior to isopropanol (Figure S6). Changing parameters under continuous-flow conditions, while monitoring the extracted ion chromatograms of key products and potential by-products, is an efficient way of following their effect on the outcome of the chemical reaction in real-time. The capacity of the system to convert lidocaine to norlidocaine was further evaluated under continuous-flow conditions at increasing lidocaine concentrations up to 1 mM. The upper concentration limit appeared to lie between 200 and 300 μM after which lidocaine started to break through resulting in a declining conversion (Figure S7). We hypothesized that this could be related to the limited availability of molecular oxygen, which has a solubility in water at ambient pressure and room temperature of about 250 μM, rather than the reactor capacity itself. This led us to study the effect of oxygen enrichment considering that gas solubility in liquids increases linearly with pressure to about 10 mM at the 40 bar pressure in the current system.

3.3. Reaction mechanism

The reaction mechanism depicted in Scheme 2, which is based on the reaction mechanism of Cytochrome P450-catalyzed dealkylations as postulated by Ren et al. [13], requires activation of molecular oxygen on the gold surface as the initial reaction step.

Molecular oxygen has also been implicated in reactions catalyzed by gold nanoparticles [17–19]. We therefore studied the role of molecular oxygen in the dealkylation reaction by removing dissolved molecular oxygen from the eluent using sulfite as pump 1 additive (Fig. 1), which oxidizes readily to sulfate (Equation (1)). The fact that there was no conversion under these conditions supports the critical role of dissolved molecular oxygen for the dealkylation reaction. Since gold is, however, known to bind a wide range of sulfur-containing compounds including sulfite and sulfate [20], sulfite may have poisoned the catalyst preventing the conversion of lidocaine to norlidocaine. We therefore also established a system to enrich the eluent with molecular oxygen generated from H_2O_2-sandwiched plug flow injections with a MnO_2- and the Au-reactor in series (Fig. 1, Equation (2)). Since this adjusted configuration increased the conversion capacity of the Au-reactor by more than one order of magnitude using up to 1 mM lidocaine (Figure S8, blue versus gray line) this demonstrates that the level of dissolved molecular oxygen is a limiting factor. No conversion was observed when omitting the Au-reactor and running sandwiched injections over the MnO_2-reactor alone. Direct sandwich injections over the Au-reactor initially showed also a slightly enhanced conversion, which decreased rapidly at plug flow volumes above 2 μL (Figure S8, orange line) indicating a transient, less efficient molecular oxygen production from H_2O_2 decomposition by this reactor alone. These results

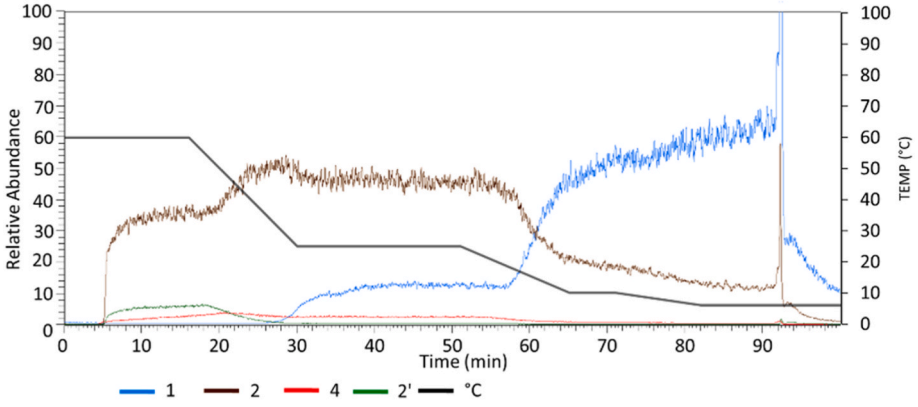

Fig. 3. Evaluation of the effect of reactor temperature (black trace) on the deethylation of lidocaine in real-time using an online MS-coupled continuous-microflow reactor monitoring the extracted ion signals of lidocaine (1), norlidocaine (2), cyclized lidocaine (4) and di-deethylated lidocaine (2′) during a 10 μM lidocaine feed at 20 μL/min (between 5 and 92 min) followed by cleaning with 0.1% formic acid in acetonitrile.

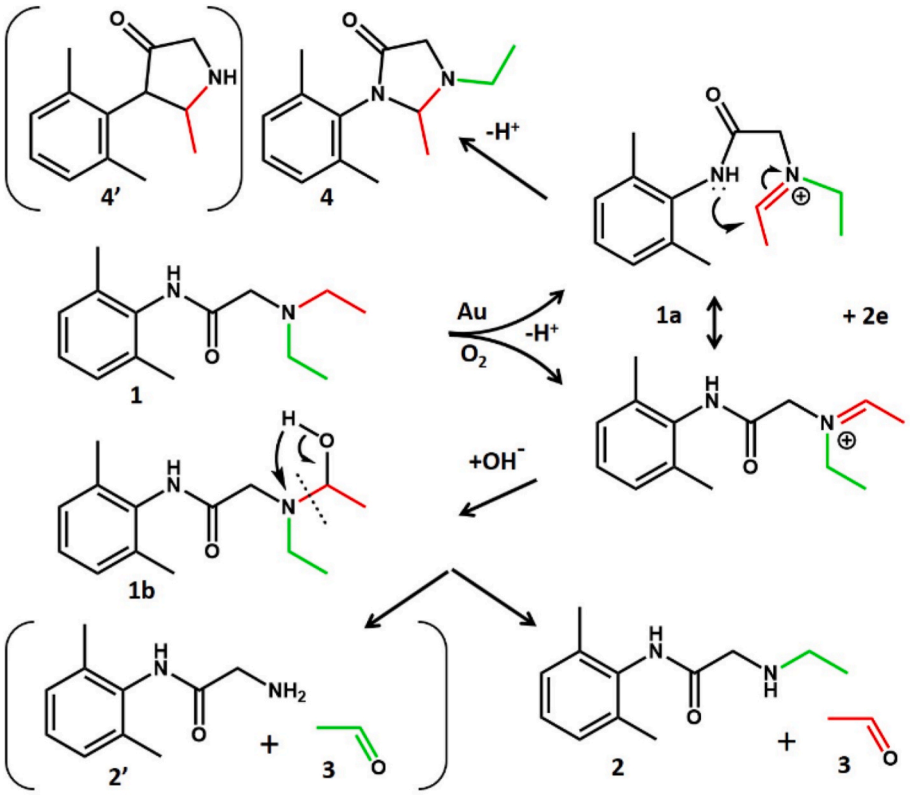

Scheme 2. Proposed reaction mechanism for the catalytic deethylation of lidocaine (1) on gold particles mainly forming norlidocaine (2) and acetaldehyde (3) via hydrolysis of a reactive iminium ion intermediate (1a) (based on Ren et al. [11]) next to a cyclized variant (4). The alkyl chains are shown in red and green, respectively, while the bracketed structures indicate side products 4′ and 2′ in case the reaction proceeds further.

illustrate that molecular oxygen is indispensable for conversion. Remarkably, generating oxygen continuously by leading H_2O_2 over the MnO_2-reactor using a fourth pump and mixing it afterwards into the sample feed ahead of the Au-reactor with a T-connector, as depicted in Figure S1, did not lead to an increased conversion capacity. The lag time before mixing with the main stream at the T-union is between 0.25 and 1 min based on a void volume of 1 μL and flow-rates between 1 and 4 μL/min. This indicates that short-lived, reactive oxygen species (ROS) play a role in the Au-catalyzed dealkylation reaction as postulated by others for oxidation reactions on heterogeneous catalysts [21–23]. He et al. [24] used electron spin resonance spectroscopy to show hydroxyl radical formation on catalytic gold nanoparticles due to H_2O_2 decomposition under acidic conditions, while molecular oxygen was generated under basic conditions, as used in our experiments (pH 8). Yan et al. [25] reported that the presence of radicals as well as water improves the adsorption and dissociation of molecular oxygen dramatically, especially on gold surfaces. This effect may also occur in our case when the substrate is sandwiched between the H_2O_2 plugs and thus intensely mixed during transport through both reactors (Fig. 1). We hypothesize that molecular oxygen, activated on the gold surface, is indispensable as electron acceptor to initiate the dealkylation reaction leading to formation of the iminium ion intermediate (Scheme 2), which is then hydrolyzed by water with concomitant incorporation of one oxygen atom into acetaldehyde.

Fig. 2 illustrates that, depending on the conditions, two by-products were detected by MS, supporting the reaction mechanism depicted in Scheme 2. The mechanism proposes two reactive intermediates (1a) and (1b) that were not detected by MS, most likely due to their short lifetimes. The reaction starts with the abstraction of H^+ from the α-carbon of the ethyl group resulting in the formation of an iminium ion (1a) while releasing two electrons. The iminium ion intermediate reacts with water via α-carbon hydroxylation (1b), a well-known reaction for enzymatic secondary and tertiary amine oxidations [26], followed by elimination of acetaldehyde (3) producing norlidocaine (2). This mechanism has also been described for electrochemical oxidation reactions, potentially producing additional hydroxylated by-products [27–29] that were not detected in our set-up.

Since acetaldehyde formation is postulated based on this reaction mechanism, we developed a post-catalyst online reactor based on the reaction between aldehydes and sulfite (2.6.3) resulting in a sulfonated product (Eq (3) that can be detected by negative ionization electrospray mass spectrometry (Figure S9, upper trace). When performing the deethylation reaction in ^{18}O-labelled water, ^{18}O was incorporated into the newly formed acetaldehyde confirming the role of water in the hydrolysis of the iminium ion intermediate (see Scheme 2). A small percentage of the iminium ion intermediate reacts intramolecularly to compound (4), as confirmed by MS (see Fig. 2). This substance has also been observed upon catalytic deethylation of lidocaine on nanoporous gold in a batch cell set-up, as confirmed by MS and NMR [12].

Taken together, our results provide strong evidence for the essential role of molecular oxygen and demonstrate the suitability of the experimental set-up to study mechanistic aspects of the dealkylation reaction.

3.4. Adsorption/desorption

Another advantage of an on-line coupled catalyst-MS system is that adsorption and desorption profiles can be recorded in real-time for a variety of chemical species. Adsorption of the substrate on the catalyst surface is considered an essential step for catalysis to occur [19,30]. Studying adsorption by frontal analysis to determine adsorption isotherms is widely used in chromatography [31–33]. While frontal analysis is not directly applicable to heterogeneous catalysts due the fact that adsorbed molecules are converted resulting in changing concentration profiles of substrate and products during their transport through the

reactor, peak shapes and slopes of the extracted ion signals provide qualitative indicators of adsorption and desorption kinetics, the strength of the interaction and possibly the existence of multiple binding/catalytic sites.

The presence of lidocaine in the cleaning fraction after a run indicated that part of it is strongly adsorbed on the gold surface without being converted (see Fig. 2b, blue bars and Figure S6, black trace). Continuous flow experiments showed that the strongly adsorbed fraction increased proportionally to the amount of lidocaine that was injected (Figure S10). A tailing norlidocaine signal after ending the substrate feed and continuing elution with water (Fig. 4, black trace) points to the existence of strong adsorption sites slowly releasing lidocaine, which is subsequently, but less efficiently, converted to norlidocaine at reactive sites along its flow path through the reactor. This suggests that an adsorptive site may not be reactive by definition. Caffeine, a compound that is neither adsorbed nor converted by the catalyst, was used as a control of the flow system showing steeply ascending and descending profiles as depicted in Fig. 4, supporting the idea that the observed peak shapes for norlidocaine are related to interaction with the catalyst surface as well as the conversion kinetics. Prolonged continuous flow experiments with the same reactor for up to 10 h showed steeper norlidocaine tails (Fig. 4, green trace), which are almost comparable to caffeine. Simultaneously, the amount of lidocaine in the cleaning fraction decreased by one order of magnitude (Figure S10, blue versus orange line), indicating saturation of the strong adsorption sites. Apparently, the catalyst surface changes with time during continuous usage. While this often diminishes the efficacy of a catalyst due to effects known as aging, fouling or poisoning as a result of multilayer formation [34], it had a positive but transient, effect in our case due to less strong adsorption leading to stable conversion. Catalyst performance deteriorated upon long-term usage (»10 h) as illustrated by a reduced norlidocaine production (blue trace in Fig. 4), making it necessary to reactivate it.

Changing surface properties are commonly observed with heterogeneous catalysts mostly due to the use of harsh preparation or regeneration conditions like annealing at high temperatures or regeneration with strong acids [34]. For example, (supported) nanoporous gold particles are subject to restructuring even during storage [35], which results in deactivation. Ultimately, the conversion efficiency of the gold particles was stable over at least 10 h producing 90% norlidocaine at a feed concentration of 10 μM lidocaine at 20 μL/min and 30 °C. It is likely that higher concentrations can be converted with oxygen enrichment and larger reactor dimensions.

4. Conclusion

We describe a modular, online microflow Au-reactor-MS system for studying the catalytic deethylation of lidocaine. This set-up allows rapid evaluation of operational parameters by following the extracted ion signals of products and by-products online, demonstrating its potential for mechanistic studies. The main limitation of the online system is the requirement to use MS-compatible solvents, reagents and additives unless a sample preparation step is included.

The instrumental configuration proved to be a flexible concept not only with respect to changing parameters such as solvents, flow-rates and temperatures but also with respect to performing pre- or post-reactor reactions. The mass spectrometric results provided direct evidence of the main conversion product as well as of by-products in support of the reaction mechanism. The presence of dissolved molecular oxygen was essential for the deethylation of lidocaine. The production of acetaldehyde and the incorporation of ^{18}O from water supported the reaction mechanism shown in Scheme 2, in which hydrolysis of the iminium ion intermediate is a necessary step. The Au-reactor showed a stable conversion efficiency of about 90% for several hours. The ascending and descending slopes of the norlidocaine signal gave qualitative insights in the surface properties of the catalyst with respect to the adsorption and desorption kinetics, as well as with respect to differences between adsorptive and reactive sites. The optimal reaction conditions for the deethylation of lidocaine are mild, using only water and molecular oxygen at or close to ambient temperature. Concentrations of up to 1 mM lidocaine were converted efficiently at 20 nmol/min when enriching the solvent with molecular oxygen by placing a MnO_2-reactor in series with the Au-catalyst and performing H_2O_2 plug-flow injections (Fig. 1). The described instrumental set-up is suitable for the study of other heterogeneous, supported homogeneous or bio-catalysts in the flow-through reactor format by screening for potential substrates and optimizing conditional parameters with a low consumption of chemicals. The simple and straightforward format using a capillary tube as reactor container is an alternative to microfluidic systems making this approach accessible to a wider range of users.

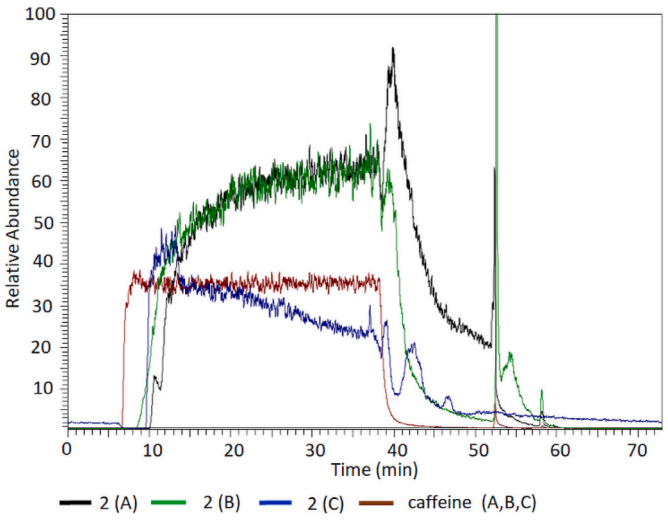

Fig. 4. Typical elution profiles of norlidocaine (2, *m/z* 207) and caffeine (*m/z* 195, brown trace), a control compound that is neither adsorbed nor converted, showing different reactivity stages of the reactor; at initial (A, black trace), 10 h (B, green trace) and »10 h usage (C, blue trace) without reactivation of the Au-reactor as assessed by a 10 μM lidocaine/caffeine feed between 5 and 37 min at 20 μL/min and 25 °C followed by 20 min water, 5 min cleaning with 0.1% formic acid in acetonitrile and 15 min reconditioning with water.

Credit author statement

Jos Hermans: Conceptualization, Methodology, Investigation, Data curation, Writing - original draft – review & editing. Ali Alipour Iranaq: Investigation - Writing - review & editing. Hjalmar Permentier: Writing - review & editing. Rainer Bischoff: Supervision, Writing - review & editing.

Declaration of competing interest

The authors declare that they have no known competing financial interests or personal relationships that could have appeared to influence the work reported in this paper.

Data availability

Data will be made available on request.

Acknowledgements

This work is part of the Open Technology Program of Toegepaste en Technische Wetenschappen (TTW) with project number 15230, which is financed by the Netherlands Organization for Scientific Research (NWO).

Appendix A. Supplementary data

Supplementary data to this article can be found online at https://doi.org/10.1016/j.talanta.2023.124928.

References

[1] J.A. Bennett, Z.S. Campbell, M. Abolhasani, Role of continuous flow processes in green manufacturing of pharmaceuticals and specialty chemicals, Curr. Opin. Chem. Eng. 26 (2019) 9–19, https://doi.org/10.1016/J.COCHE.2019.07.007.

[2] R. Ciriminna, M. Pagliaro, R. Luque, Heterogeneous catalysis under flow for the 21st century fine chemical industry, Green Energy Environ. 6 (2021) 161–166, https://doi.org/10.1016/j.gee.2020.09.013.

[3] J. Yue, J.C. Schouten, T. Alexander Nijhuis, Integration of microreactors with spectroscopic detection for online reaction monitoring and catalyst characterization, Ind. Eng. Chem. Res. 51 (2012) 14583–14609, https://doi.org/10.1021/IE301258J/ASSET/IMAGES/LARGE/IE-2012-01258J_0010 (JPEG).

[4] L.P.E. Yunker, R.L. Stoddard, J.S. McIndoe, Practical approaches to the ESI-MS analysis of catalytic reactions, J. Mass Spectrom. 49 (2014) 1–8, https://doi.org/10.1002/jms.3303.

[5] A. Ray, T. Bristow, C. Whitmore, J. Mosely, On-line reaction monitoring by mass spectrometry, modern approaches for the analysis of chemical reactions, Mass Spectrom. Rev. 37 (2018) 565–579, https://doi.org/10.1002/MAS.21539.

[6] M. Solsona, J.C. Vollenbroek, C.B.M. Tregouet, A.E. Nieuwelink, W. Olthuis, A. Van Den Berg, B.M. Weckhuysen, M. Odijk, Microfluidics and catalyst particles, Lab Chip 19 (2019) 3575–3601, https://doi.org/10.1039/C9LC00318E.

[7] H. Fleischer, V.Q. Do, K. Thurow, Online measurement system in reaction monitoring for determination of structural and elemental composition using mass spectrometry, SLAS Technol. 24 (2019) 330–341, https://doi.org/10.1177/2472630318813838.

[8] P. Khanipour, M. Löffler, A.M. Reichert, F.T. Haase, K.J.J. Mayrhofer, I. Katsounaros, Electrochemical real-time mass spectrometry (EC-RTMS): monitoring electrochemical reaction products in real time, Angew. Chem. Int. Ed. 58 (2019) 7273–7277, https://doi.org/10.1002/anie.201901923.

[9] R. Munirathinam, J. Huskens, W. Verboom, Supported catalysis in continuous-flow microreactors, Adv. Synth. Catal. 357 (2015) 1093–1123, https://doi.org/10.1002/ADSC.201401081.

[10] S.A. Shahzad, M.A. Sajid, Z.A. Khan, D. Canseco-Gonzalez, Gold catalysis in organic transformations: a review, Synth. Commun. 47 (2017) 735–755, https://doi.org/10.1080/00397911.2017.1280508.

[11] Y. Zhang, J. Zhang, B. Zhang, R. Si, B. Han, F. Hong, Y. Niu, L. Sun, L. Li, B. Qiao, K. Sun, J. Huang, M. Haruta, Boosting the catalysis of gold by O2 activation at Au-SiO2 interface, Nat. Commun. 11 (2020) 1–10, https://doi.org/10.1038/s41467-019-14241-8.

[12] A.A. Najmi, E. Jafariyeh-Yazdi, M. Hadian, J. Hermans, R. Bischoff, J. Yue, A. Dömling, A. Wittstock, H.P. Permentier, Nanoporous gold catalyst for the oxidative N-dealkylation of drug molecules: a method for synthesis of N-dealkylated metabolites, Chem. Med. Chem. (2022), e202200040, https://doi.org/10.1002/CMDC.202200040.

[13] X. Ren, J.A. Yorke, E. Taylor, T. Zhang, W. Zhou, L.L. Wong, Drug oxidation by Cytochrome P450 $_{BM3}$: metabolite synthesis and discovering new P450 reaction types, Chem. Eur J. 21 (2015) 15039–15047, https://doi.org/10.1002/chem.201502020.

[14] K.M. Roberts, Mechanistic Evaluation of N-Dealkylation by Cytochrome P450 Using N,N-Dimethylaniline N-Oxides and Kinetic Isotope Effects, Washington State University, 2009.

[15] C. Chen, J. Min, L. Zhang, Y. Yang, X. Yu, R. Guo, Advanced understanding of the electron transfer pathway of Cytochrome P450s, Chembiochem 22 (2021) 1317–1328, https://doi.org/10.1002/cbic.202000705.

[16] Y.N. Hu, D. Chen, T.Y. Zhang, J. Ding, Y.Q. Feng, Use of ammonium sulfite as a post-column derivatization reagent for rapid detection and quantification of aldehydes by LC-MS, Talanta 206 (2020), 120172, https://doi.org/10.1016/j.talanta.2019.120172.

[17] R. Pal, L.M. Wang, Y. Pei, L.S. Wang, X.C. Zeng, Unraveling the mechanisms of O 2 activation by size-selected gold clusters: transition from superoxo to peroxo chemisorption, J. Am. Chem. Soc. 134 (2012) 9438–9445, https://doi.org/10.1021/ja302902p.

[18] M.A. Dar, S. Krishnamurty, Molecular and dissociative adsorption of oxygen on Au-Pd bimetallic clusters: role of composition and spin state of the cluster, ACS Omega 4 (2019) 12687–12695, https://doi.org/10.1021/acsomega.9b01581.

[19] K.M. Kosuda, A. Wittstock, C.M. Friend, M. Bäumer, Oxygen-mediated coupling of alcohols over nanoporous gold catalysts at ambient pressures, Angew. Chem. Int. Ed. 51 (2012) 1698–1701, https://doi.org/10.1002/anie.201107178.

[20] P. Carro, R.C. Salvarezza, Gold adatoms modulate sulfur adsorption on gold, Nanoscale 11 (2019) 19341–19351, https://doi.org/10.1039/c9nr05709a.

[21] M. Ruokolainen, T. Gul, H. Permentier, T. Sikanen, R. Kostiainen, T. Kotiaho, Comparison of TiO2 photocatalysis, electrochemically assisted Fenton reaction and direct electrochemistry for simulation of phase i metabolism reactions of drugs, Eur. J. Pharmaceut. Sci. 83 (2016) 36–44, https://doi.org/10.1016/j.ejps.2015.12.012.

[22] M. Gilles, E. Brun, C. Sicard-Roselli, Quantification of hydroxyl radicals and solvated electrons produced by irradiated gold nanoparticles suggests a crucial role of interfacial water, J. Colloid Interface Sci. 525 (2018) 31–38, https://doi.org/10.1016/j.jcis.2018.04.017.

[23] M. Misawa, J. Takahashi, Generation of reactive oxygen species induced by gold nanoparticles under x-ray and UV Irradiations, Nanomed. Nanotechnol. Biol. Med. 7 (2011) 604–614, https://doi.org/10.1016/j.nano.2011.01.014.

[24] W. He, Y.T. Zhou, W.G. Wamer, X. Hu, X. Wu, Z. Zheng, M.D. Boudreau, J.J. Yin, Intrinsic Catalytic Activity of Au Nanoparticles with Respect to Hydrogen Peroxide Decomposition and Superoxide Scavenging, Biomaterials, 2013, https://doi.org/10.1016/j.biomaterials.2012.10.010.

[25] M. Yan, Z.Q. Huang, Y. Zhang, C.R. Chang, Trends in water-promoted oxygen dissociation on the transition metal surfaces from first principles, Phys. Chem. Chem. Phys. 19 (2017) 2364–2371, https://doi.org/10.1039/c6cp06974f.

[26] J. Rose, N. Castagnoli, The metabolism of tertiary amines, Med. Res. Rev. 3 (1983) 73–88, https://doi.org/10.1002/MED.2610030105.

[27] E. Nouri-Nigjeh, H.P. Permentier, R. Bischoff, A.P. Bruins, Electrochemical oxidation by square-wave potential pulses in the imitation of oxidative drug metabolism, Anal. Chem. 83 (2011) 5519–5525, https://doi.org/10.1021/ac200897p.

[28] E. Nouri-Nigjeh, H.P. Permentier, R. Bischoff, A.P. Bruins, Lidocaine oxidation by electrogenerated reactive oxygen species in the light of oxidative drug metabolism, Anal. Chem. 82 (2010) 7625–7633, https://doi.org/10.1021/ac101364s.

[29] T. Gul, R. Bischoff, H.P. Permentier, Mechanism of aromatic hydroxylation of lidocaine at a Pt electrode under acidic conditions, Electrochim. Acta 224 (2017) 636–641, https://doi.org/10.1016/j.electacta.2016.12.089.

[30] E. Roduner, Understanding catalysis, Chem. Soc. Rev. 43 (2014) 8226–8239, https://doi.org/10.1039/c4cs00210e.

[31] O. Lisec, P. Hugo, A. Seidel-Morgenstern, Frontal analysis method to determine competitive adsorption isotherms, J. Chromatogr., A 908 (2001) 19–34, https://doi.org/10.1016/S0021-9673(00)00966-3.

[32] J. Jacobson, J. Frenz, C. Horváth, Measurement of adsorption isotherms by liquid chromatography, J. Chromatogr., A 316 (1984) 53–68, https://doi.org/10.1016/S0021-9673(00)96140-5.

[33] N. Marchetti, A. Cavazzini, L. Pasti, F. Dondi, Determination of adsorption isotherms by means of HPLC: adsorption mechanism elucidation and separation optimization, J. Separ. Sci. 32 (2009) 727–741, https://doi.org/10.1002/jssc.200800425.

[34] C.H. Bartholomew, M.D. Argyle, Advances in catalyst deactivation and regeneration, Catalysts 5 (2015) 949–954, https://doi.org/10.3390/catal5020949.

[35] R. Zanella, C. Louis, Influence of the conditions of thermal treatments and of storage on the size of the gold particles in Au/TiO2 samples, in: Catal. Today, Elsevier, 2005, pp. 768–777, https://doi.org/10.1016/j.cattod.2005.07.008.